Structural Engineering and Mechanics, *Vol. 56, No. 3 (2015) 385-407*
DOI: http://dx.doi.org/10.12989/sem.2015.56.3.385

Structural system simulation and control via NN based fuzzy model

Pei-Wei Tsai[1,2], T. Hayat[3,4], B. Ahmad[4] and Cheng-Wu Chen[*2,5]

[1]*College of Information Science and Engineering, Fujain University of Technology, Fuzhou, China*
[2]*Department of Maritime Information and Technology, National Kaohsiung Marine University, Kaohsiung, Taiwan, R.O.C.*
[3]*Department of Mathematics, Quaid-I-Azam University 45320, Islamabad 44000, Pakistan*
[4]*Nonlinear Analysis and Applied Mathematics (NAAM) Research Group, Department of Mathematics, Faculty of Science, King Abdulaziz University, Jeddah 21589, Saudi Arabia*
[5]*Faculty of Engineering, King Abdulaziz University, Jeddah 21589, Saudi Arabia*

(Received April 18, 2014, Revised October 19, 2015, Accepted October 20, 2015)

Abstract. This paper deals with the problem of the global stabilization for a class of tension leg platform (TLP) nonlinear control systems. It is well known that, in general, the global asymptotic stability of the TLP subsystems does not imply the global asymptotic stability of the composite closed-loop system. Finding system parameters for stabilizing the control system is also an issue need to be concerned. In this paper, we give additional sufficient conditions for the global stabilization of a TLP nonlinear system. In particular, we consider a class of NN based Takagi-Sugeno (TS) fuzzy TLP systems. Using the so-called parallel distributed compensation (PDC) controller, we prove that this class of systems can be globally asymptotically stable. The proper design of system parameters are found by a swarm intelligence algorithm called Evolved Bat Algorithm (EBA). An illustrative example is given to show the applicability of the main result.

Keywords: linear matrix inequality; automated design; fuzzy logic model and control; Evolved Bat Algorithm

1. Introduction

The wave-structure interaction problem has been investigated by researchers for decades. The demands for the products of natural energy resources have been rapidly increasing in recent years motivating companies to go to more remote places such as beneath deeper oceans to obtain these resources. The tension Leg Platform (TLP) is an artificial structure commonly found in the ocean or near the coast, where the natural resources such as the gas and the oil exists (Lee and Juang 2012). It is particularly suited for drilling at water depths greater than 300 meters. The platform is permanently moored by tethers or tendons grouped at each of the structure's corners. Regardless of whether the TLP is built in the middle of the ocean or near the coast, it is subject to the constant impact of wind and waves. A TLP built near the coast not only receives the impact from

∗Corresponding author, Professor, E-mail: chengwu@mail.nkmu.edu.tw

http://www.techno-press.org/?journal=sem&subpage=8 ISSN: 1225-4568 (Print), 1598-6217 (Online)

the waves, but also has to resist the energy from reflection rebounding back from the coast. The force caused by the wave effect can be treated as a nonlinear system; and the force generated by the reflection effect can be treated as a time-delay problem. Due to the huge investment for the development of TLPs, there is interest in the study of the dynamic responses of such structures under external wave excitations. The TLP can be damaged if the vibration or the response is too strong. This study proposes some structural stability modeling methods for considering the influence of external waves on these oceanic structures. The external forces of concern for structures such as bridges are wind forces, earthquakes excitation and external disturbances. In order to ensure the TLP system is stable in the large, an active stabilizer can be applied to generate the resistance force against forces from waves and reflections. Moreover, a fuzzy controller can be employed to create the control scheme for holding the TLP in a stable position. In this paper, we propose a Neural Network (NN) based fuzzy model to decompose the temporal state of the nonlinear system and utilize Evolved Bat Algorithm (EBA) to determine the system parameters and the scale of the control force needed for stabilizing the TLP system. In the stabilization analysis, the Linear Matrix Inequality (LMI) condition is derived by the Lyapunov theory to guarantee the system stability and produce an automated design for a nonlinear system. Base on the stability analysis, the stability of an oceanic TLP structure can be proved theoretically. The fuzzy and neural network modeling methods are proposed for decomposing the nonlinear system at the beginning. Moreover, the stability criterion can be derived from the decomposed time-delayed TLP system via the Lyapunov theory with the LMI conditions. In addition, the swarm intelligence method called the EBA is used to find feasible solutions and the proper controller force under the stability criteria derived above. Finally, the displacement decay due to the use of the proposed NN modeling design and controllers are demonstrated in a numerical simulation.

2. Literature review

Several method for evaluating stability designs have been successfully applied (Loria and Nesic 2003, Mazenc *et al*. 1999, Panteley and Loria 1998, Sontag 1988, Sontag and Wang 1995). Computational intelligence approaches such as neural networks and fuzzy systems have also been used to model dynamic phenomena and applications in different areas. These tools have proven to be powerful and effective. Several of the more recent works using these approaches can also be seen. On the other hand, algorithms in swarm intelligence are also widely used to construct the simulation model of a system or to provide optimal solutions for problems in manufacturing, scheduling, and logistics in business, finance, and engineering. For instant, Cat Swarm Optimization (CSO) is utilized to develop a set of population based learning rules for an Infinite Impulse Response (IIR) system (Panda *et al*. 2011) and can also be used to solve multiple objective problems (Pardhan and Panda 2012). In addition, CSO has been utilized to optimize the information hiding results (Wang *et al*. 2012); Interactive Artificial Bee Colony (IABC) is successfully used to improve the recognition rate of the continuous authentication system (Tsai *et al*. 2012) and to forecast the trends of the foreign exchange rate (Chang *et al*. 2014); and Evolved Bat Algorithm (EBA) has been employed to illustrate its usability in providing the optimal recommended stock portfolio (Chang *et al*. 2014).

Although there have been many successful applications of intelligent computation, there are still some drawbacks to using them in any control scheme. To the best of our knowledge, the analysis

of stability of TLPs with the NN-fuzzy model has not yet been discussed. For this reason, a fuzzy Lyapunov method as well as a NN-fuzzy model for dealing with the stability problem of TLPs (Lam 2009, Lee *et al*. 2001, Liu and Zhang 2003, Park *et al*. 2003, Tanaka *et al*. 1994, Wang *et al*. 1996) is given at the beginning. From this we study suitable mathematical modeling for the TLP system and discuss the interaction between a deformable floating structure and surface wave motion by virtue of a partial differential equation as well as fuzzy logic theory.

Egresits *et al*. professed intelligence is strongly connected with learning adapting abilities, consequently such capabilities are considered as indispensable features of intelligent manufacturing systems (Chu and Tsai 2007). A number of approaches have been portrayed to apply different machine learning techniques for manufacturing problems, starting with rule induction in symbolic pattern and domains recognition techniques in numerical, sub symbolic domains. Artificial neural network (ANN) based learning is the dominant machine learning technique in manufacturing in recent years. It can not only be used in classification, and estimation, but can also be employed for stability analysis. For example, the nonlinear Markov jump standard genetic regulatory network model can be constructed using the recurrent neural networks (Zhu *et al*. 2013). However, mainly these solutions have limited industrial acceptance because of the 'black box' nature of ANNs. The integration of neural and fuzzy techniques is treated and former solutions are analyzed in (Egresits *et al*. 1998). Narendra *et al*. (1998) portrayed an intelligent current controller for the fast and flexible control using ANN and Fuzzy Logic paradigms (Lian *et al*. 1998). Two methods of adjusting the learning parameters are presented: A heuristic approach to evaluate the learning rate as a polynomial of an energy function is considered and learning parameters are discussed; on the other hand, Fuzzy logic, genetic algorithms and neural networks are three popular artificial intelligence techniques which are used in many applications widely (Lian *et al*. 1998). Owing to their distinct properties and advantages, they are being investigated and integrated to form new models or strategies in the areas of system control currently. A linear mapping method is used to encode the GA chromosome, which comprises the center and width of the membership functions, and also the weights of the controller. Dynamic crossover and mutation probabilistic rates are also applied for faster convergence of the GA evolvement. Kuo and Xue endeavored to develop an intelligent sales forecasting system which can consider the quantitative factors as well as the non-quantitative factors (Kuo and Xu 1998). The proposed forecasting system comprises data collection, general pattern model, special pattern model, and decision integration. A feed forward neural network with error-back propagation (EBP) learning algorithm is employed to learn the time series data, or quantitative factors in the general pattern model. This paper utilized fuzzy logic which is capable of learning to learn the experts' knowledge considering the effect of promotion on the sales. In recent years, the research interest regarding GRNs is also increasing (Lee and Juang 2012, Lewandowski *et al*. 2012). By using a constellation of artificial intelligence technologies, electronic Warfare (EW) Support Measures (ESM) systems are evolving rapidly toward unmanned status (Sciortino 1997). The implementation and applications techniques, for which adaptive self-governing non-cooperative target recognition is useful or necessary, form the focus of this discussion. Military and civilian applications abound for fixed site, ship borne, and airborne systems. These systems could control and manage other interactive systems normally needing manual inputs. Simoes *et al*. portrayed the control strategy development, experimental performance, and design e evaluation of a fuzzy-logic-based variable-speed wind generation system that uses a cage-type induction generator and double-sided pulse width-modulated converters (Simoes *et al*. 1997). The system can feed a utility grid maintaining unity power factor at all conditions or can supply a self-governing load.

The fuzzy-logic-based control of the system helps to optimize efficiency and improve performance. In metal processing industries, Grauel *et al*. compared three computer-aided systems used for quality monitoring and on-line process (Grauel *et al*. 1997). From which significant quality statements are extracted in a running manufacturing process measurement data are taken. For this they applied on one hand an artificial neural network, which learns to categorize the data adequately by using given exemplary process states. Besides, they presented investigations of fuzzy clustering techniques to acquire information about the process. Furthermore, topology optimization by evolutionary algorithms is considered to acquire optimal structures of the multilayer perception used. On to the next hierarchical level, the quality features extracted are then passed, where they are processed within the framework of an integrated manufacturing and quality control system. Yen proposed to design and to evaluate an on-board intelligent health assessment tool for rotorcraft machines, which is capable of discovering, recognizing, and accommodating expected system degradations and unanticipated catastrophic failures in rotorcraft machines under an adverse operating environment (Yen 1996). A fuzzy-based neural network paradigm with an on-line learning algorithm is developed to execute expert advising for the ground-based maintenance crew. Hierarchical fault diagnosis architecture is advocated to perform on-board needs and the time-critical in different levels of structural integrity over a global operating envelope. In modern process automation, intelligent control has become a question of primary importance as it provides the prerequisites for the task of fault detection (Tyan *et al*. 1996). The ability to detect the faults is important to improve reliability and security of a complex control system. During recent years, parameter estimation methods, state observation schemes, statistical likelihood ratio tests, rule-based expert system reasoning, pattern recognition techniques, and artificial neural network approaches are the most common methodologies developed actively. Tyan *et al*. described a completed feasibility study demonstrating the merit of employing pattern recognition and an artificial neural network for error diagnosis through back propagation learning algorithm and making the use of fuzzy approximate reasoning for fault control via parameter changes in a dynamic system (Tyan *et al*. 1996).

Some references of damage assessment and uncertainty analysis were published to mitigate the threaten of casualty, in which the fuzzy theory has received considerable attention recently in structural engineering. Various approaches have been developed for detecting damage based on various methods (Egresits *et al*. 1998, Hammami 2001, Ignaciuk and Bartoszewicz 2010, Korkmaz 2011, Kuok *et al*. 2012).

For intricate dynamical systems, in designing controllers there are needs that are not sufficiently addressed by conventional control theory (Tyan *et al*. 1996). These relate mainly to the problem of environmental uncertainty and often call for human-like decision making needing the use of heuristic reasoning and learning experience. Learning is needed complexity of a problem or the uncertainty thereof prevents a priori specification of a satisfactory solution. Such solutions are then only possible through gathering information about the problem and using this information to dynamically generate an acceptable solution. Such systems can be referred to as intelligent control systems. Buss and Hashimoto tried to summarize the field of intelligent control for human-machine systems from a subjective point of view (Buss and Hashimoto 1996). From integrating mechanical, software and electrical intelligence in minimum space, mechatronic components have become intelligent, certainly an important step. With a bright future, taking this and recent successes using artificial neural networks, fuzzy logic and genetic algorithms, so called soft computing, the field of IC is exciting. This article attempts to expect this future and discusses directions of research to approach the realization of more intelligent systems.

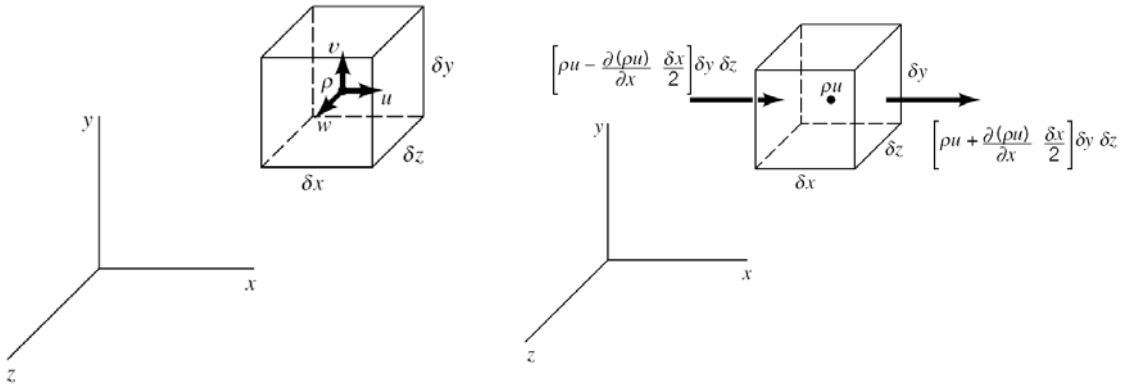

Fig. 1 A differential element for the development of the conservation of mass equation

2. Mathematical formulation

2.1 Initial boundary value problem for fluid–structure interaction

Fig. 1(a) shows a drawing of a stationary cubical element. The mass inside a fixed surface bounding a closed volume will increase if mass flows into the volume and decrease if it flows out. The inflow and outflow processes are shown in Fig. 1(b). For incompressible fluids the fluid density is constant throughout the flow field. Thus

$$\nabla \cdot \vec{\mathrm{V}} = 0 \tag{1}$$

Here, the fluid is considered inviscid, and the flow is assumed to move from rest so that it is irrotational. Therefore, the fluid velocity $\vec{\mathrm{V}}$ can be described by the gradient of the velocity potential $\boldsymbol{\Phi}(x,z,t)$ in the fluid domain, i.e., $\vec{\mathrm{V}} = \nabla\Phi(x,z,t)$. The governing equation for this problem satisfies the Laplace equation for the velocity potential, i.e.

$$\nabla^2\Phi(x,z,t) = 0 \tag{2}$$

The derivations for the fluid domain equations are based on the following assumptions:

1. The fluid is considered inviscid.
2. The flow is incompressible and irrotational, so surface tension effects can be neglected.
3. The flow can be described by the scalar velocity potential satisfying the Laplace equation within the fluid domain.
4. No breaking waves occur on the sea surface.

Consider a wave-induced flow field system in which a Cartesian coordinate system *oxz* is employed. As shown in the sketch of a 2D numerical wave flume, a plane z=0 coincides with the undisturbed still water level and the z-axis is directed vertically upward. The vertical elevation of any point on the free surface can be defined by the function $z=\eta(x,y,t)$, in which the surface tension is negligible. As depicted in Fig. 2, $-\infty<x<-b$, where the total velocity potential Φ_I in Region I consists of incident waves Φ_i , scattered waves Φ_{IS} and motion radiation waves Φ_{IW}. In Region II,

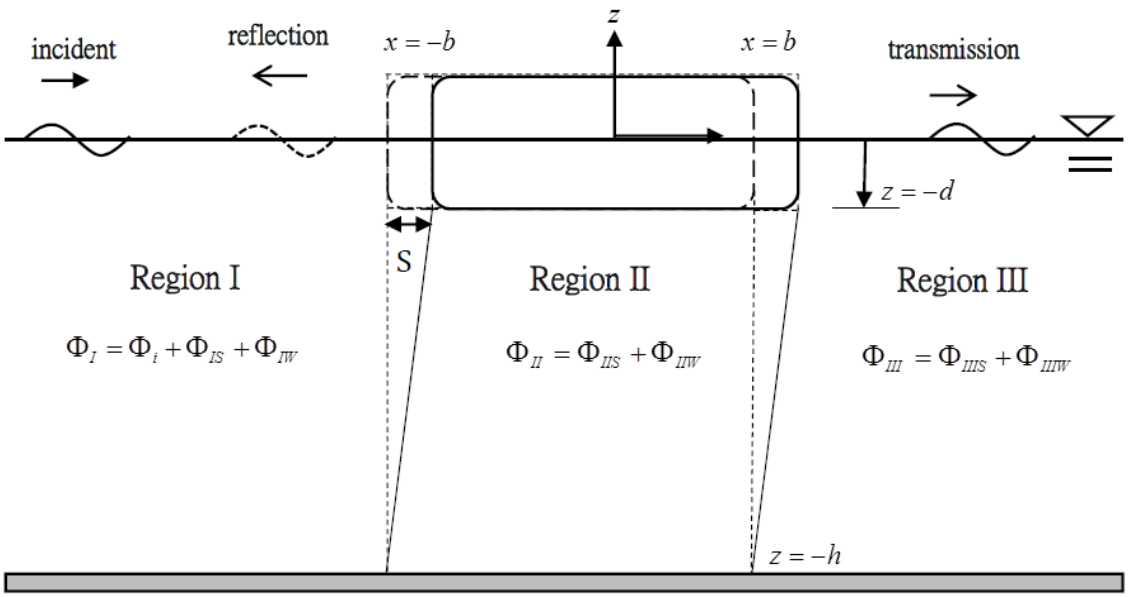

Fig. 2 Sketch defining a deformable tension leg platform subjected to the wave force

$-b<x<b$, and in Region III, $b<x<\infty$; the total velocity potentials Φ_{II} and Φ_{III} consist of both scattered Φ_{IIS} and Φ_{IIIS} and radiated waves Φ_{IIW} and Φ_{IIIW}. Subscript S denotes the scattering problem and subscript W denotes the wave-maker (i.e., primitive radiation) problem induced by the platform surge motion. Displacement of the surge motion with an unknown amplitude S is given by $\overline{X} = Se^{-i\sigma t}$ and platform deformation on the x-axis is defined as S.

It is assumed that there is no flow across any fluid interface, in other words, fluid particles can only move in a direction tangential to the fluid interface. The required kinematic boundary conditions are as follows

$$\frac{\partial \eta}{\partial t} = \frac{\partial \Phi}{\partial z} - \frac{a}{\lambda}\frac{\partial \Phi}{\partial x}\frac{\partial \eta}{\partial x} \quad \text{on the free surface} \tag{3}$$

$$\frac{\partial \Phi}{\partial n} = U_n \quad \text{on the rigid boundaries} \tag{4}$$

where $a<<\lambda$ for small-amplitude waves and we can neglect the non-linear convective term; and n is the outward normal to the boundary. Furthermore, the application of the linearized condition at $z=0$ instead of $z=\eta$ results in the kinematic boundary condition $\partial\eta/\partial t=w$, suggesting that the vertical velocity component of the fluid at the interface must be equal to the interface velocity. When the rigid boundaries are stationary on the seabed, the normal velocity component U_n becomes zero.

The dynamic boundary condition on the free surface is utilized to calculate the dynamic pressure and horizontal fluid velocity. The dynamic conditions on the free surface are derived based on the conservation of linear momentum. Briefly, the discontinuity in the normal stress is proportional to the mean curvature of the free surface caused by surface tension

$$\frac{\partial \Phi}{\partial t} = C - g\eta - \frac{1}{2}\left[\left(\frac{\partial \Phi}{\partial x}\right)^2 + \left(\frac{\partial \Phi}{\partial z}\right)^2\right] - \frac{P}{\rho} \tag{5}$$

where C is the Bernoulli constant. When the atmospheric pressure is zero, term P will also be equal to zero. In free-surface problems, nonlinearity in the potential flow problem is only derived from free-surface boundary conditions when inviscid and incompressible fluid and irrotational flow assumptions are made. For small amplitude waves, the high order terms in the free surface boundary conditions given by Eqs. (3) and (5) are ignored, and the resulting conditions are applied at the undisturbed water level: z=0 with C=0. The following expression is obtained

$$\eta = -\frac{1}{g}\frac{\partial \Phi}{\partial t} \tag{6}$$

The Sommerfeld radiation condition is utilized as the outflow boundary condition with no interference inside the computational domain

$$\lim_{x \to \pm\infty}\left[\frac{\partial \Phi_{IS/IIIS}}{\partial x} \pm \frac{1}{c}\frac{\partial \Phi_{IS/IIIS}}{\partial t}\right] = 0 \tag{7}$$

2.2 Boundary value problem for each region

Based on this description we obtain the governing equations and boundary conditions for the three regions.

2.2.1 Region I

Governing equations

$$\begin{cases} \nabla^2 \Phi_{IS} = 0 \\ \nabla^2 \Phi_{IW} = 0 \end{cases} \tag{8}$$

Kinematic boundary conditions

$$\begin{cases} \dfrac{\partial \Phi_{IS}}{\partial z} = \dfrac{\partial \eta_{IS}}{\partial t} \\ \dfrac{\partial \Phi_{IW}}{\partial z} = \dfrac{\partial \eta_{IW}}{\partial t} \end{cases} \quad \text{on} \quad z = 0 \tag{9}$$

$$\begin{cases} \dfrac{\partial \Phi_{IS}}{\partial z} = 0 \\ \dfrac{\partial \Phi_{IW}}{\partial z} = 0 \end{cases} \quad \text{on} \quad z = -h \tag{10}$$

$$\begin{cases} \dfrac{\partial \Phi_{IS}}{\partial x} = 0 & -d \le z \le 0 \\ \dfrac{\partial \Phi_{IW}}{\partial x} = \dfrac{\partial \xi}{\partial t} & -d \le z \le 0 \\ \dfrac{\partial \Phi_{IS}}{\partial x} = \dfrac{\partial \Phi_{IIS}}{\partial x} & -h \le z \le -d \\ \dfrac{\partial \Phi_{IW}}{\partial x} = \dfrac{\partial \Phi_{IIW}}{\partial x} & -h \le z \le -d \end{cases} \quad \text{on } x = -b \tag{11}$$

Dynamic boundary conditions

$$\begin{cases} \eta_{IS} = -\dfrac{1}{g}\dfrac{\partial \Phi_{IS}}{\partial t} \\ \eta_{IW} = -\dfrac{1}{g}\dfrac{\partial \Phi_{IW}}{\partial t} \end{cases} \quad \text{on} \quad z = 0 \tag{12}$$

$$\begin{cases} \dfrac{\partial \Phi_{IS}}{\partial t} = \dfrac{\partial \Phi_{IIS}}{\partial t} & -h \le z \le -d \\ \dfrac{\partial \Phi_{IW}}{\partial t} = \dfrac{\partial \Phi_{IIW}}{\partial t} & -h \le z \le -d \end{cases} \quad \text{on} \quad x = -b \tag{13}$$

Radiation condition

$$\lim_{x \to -\infty} \left[\frac{\partial \Phi_{IS}}{\partial x} - \frac{1}{c}\frac{\partial \Phi_{IS}}{\partial t} \right] = 0 \tag{14}$$

2.2.2 Region II

Governing equations

$$\begin{cases} \nabla^2 \Phi_{IIS} = 0 \\ \nabla^2 \Phi_{IIW} = 0 \end{cases} \tag{15}$$

Kinematic boundary conditions

$$\begin{cases} \dfrac{\partial \Phi_{IIS}}{\partial z} = 0 \\ \dfrac{\partial \Phi_{IIW}}{\partial z} = 0 \end{cases} \quad \text{on} \quad z = -d \tag{16}$$

$$\begin{cases} \dfrac{\partial \Phi_{IIS}}{\partial z} = 0 \\ \dfrac{\partial \Phi_{IIW}}{\partial z} = 0 \end{cases} \quad \text{on} \quad z = -h \tag{17}$$

Dynamic boundary condition

$$gd = \frac{\partial(\Phi_{IIS} + \Phi_{IIW})}{\partial t} + \frac{P}{\rho} \quad \text{on} \quad z = -d \tag{18}$$

2.2.3 Region III

Governing equations

$$\begin{cases} \nabla^2 \Phi_{IIIS} = 0 \\ \nabla^2 \Phi_{IIIW} = 0 \end{cases} \tag{19}$$

Kinematic boundary conditions

$$\begin{cases} \dfrac{\partial \Phi_{IIIS}}{\partial z} = \dfrac{\partial \eta_{IIIS}}{\partial t} \\ \dfrac{\partial \Phi_{IIIW}}{\partial z} = \dfrac{\partial \eta_{IIIW}}{\partial t} \end{cases} \quad \text{on} \quad z = 0 \tag{20}$$

$$\begin{cases} \dfrac{\partial \Phi_{IIIS}}{\partial z} = 0 \\ \dfrac{\partial \Phi_{IIIW}}{\partial z} = 0 \end{cases} \quad \text{on} \quad z = -h \tag{21}$$

$$\begin{cases} \dfrac{\partial \Phi_{IIIS}}{\partial x} = 0 & -d \le z \le 0 \\ \dfrac{\partial \Phi_{IIIW}}{\partial x} = \dfrac{\partial \xi}{\partial t} & -d \le z \le 0 \\ \dfrac{\partial \Phi_{IIIS}}{\partial x} = \dfrac{\partial \Phi_{IIS}}{\partial x} & -h \le z \le -d \\ \dfrac{\partial \Phi_{IIIW}}{\partial x} = \dfrac{\partial \Phi_{IIW}}{\partial x} & -h \le z \le -d \end{cases} \quad \text{on} \quad x = b \tag{22}$$

Dynamic boundary conditions

$$\begin{cases} \eta_{IIIS} = -\dfrac{1}{g}\dfrac{\partial \Phi_{IIIS}}{\partial t} \\ \eta_{IIIW} = -\dfrac{1}{g}\dfrac{\partial \Phi_{IIIW}}{\partial t} \end{cases} \quad \text{on} \quad z = 0 \tag{23}$$

$$\begin{cases} \dfrac{\partial \Phi_{IIIS}}{\partial t} = \dfrac{\partial \Phi_{IIS}}{\partial t} & -h \le z \le -d \\ \dfrac{\partial \Phi_{IIIW}}{\partial t} = \dfrac{\partial \Phi_{IIW}}{\partial t} & -h \le z \le -d \end{cases} \quad \text{on} \quad x = b \tag{24}$$

Radiation condition

$$\lim_{x\to+\infty}\left[\frac{\partial \Phi_{IIIS}}{\partial x}+\frac{1}{c}\frac{\partial \Phi_{IIIS}}{\partial t}\right]=0 \tag{25}$$

In the following, the LDI representation representing the TLP system will be introduced and the stability criterion derived.

2.3 Swarm intelligence method: Evolved Bat Algorithm (EBA)

The field of swarm intelligence includes various algorithms inspired by tinny intelligent from creatures in the Mother Nature. Several algorithms in swarm intelligence are proposed one after another. Most of the algorithms are developed by imitating behaviors or the particular survival skills of creatures. For example, Tsai *et al*. proposes a newly developed swarm intelligence algorithm called Evolved Bat Algorithm (EBA) in the late 2011 (Tsai *et al*. 2012). EBA is an algorithm inspired by the theory of the bat echolocation in the natural world. Different from other swarm intelligence algorithms such as Particle Swarm Optimization (PSO) (Eberhart and Kennedy 1995), Artificial Bee Colony (ABC) optimization (Karaboga 2005, Karaboga and Basturk 2008), or Cat Swarm Optimization (CSO) (Chu and Tsai 2007, Chu *et al*. 2006), only one parameter, the medium, should be determined before employing EBA. The chosen medium determines the step size of the movement of the artificial agent in the solution space. In general, the step size has a direct influence on the search results. Properly select the parameter results in the suitable step size for the artificial agents to move in the solution space. It implies that the accuracy of finding the near best solutions is raised and the possibility of trapping in the local optimum is reduced. In our experiment, the chosen medium is air for the reason that air is the original existence medium in the natural environment in where bats live. The operation of EBA is briefly reviewed as follows:

Step 1. **Initialization**: the artificial agents are spread into the solution space by randomly assigning coordinates to them.

Step 2. **Movement**: the artificial agents are moved according to Eqs. (26)-(27). A random number is generated and then it is checked whether it is greater than the fixed pulse emission rate. If the result is positive, the artificial agent is moved using the random walk process, as defined by Eq. (28).

$$x_i^t = x_i^{t-1} + D \tag{26}$$

where x_i^t indicates the coordinate of the i^{th} artificial agent at the t^{th} iteration, x_i^{t-1} represents the coordinate of the i^{th} artificial agent at the last iteration, and D is the moving distance that the artificial agent goes in this iteration.

$$D = \gamma \cdot \Delta T \tag{27}$$

where γ is a constant corresponding to the medium chosen in the experiment, and $\Delta T \in [-1.1]$ is a random number. γ=0.17 is used in our experiment because the chosen medium is air.

$$x_i^{t_R} = \beta \cdot \left(x_{best} - x_i^t\right), \quad \beta \in [0,1] \tag{28}$$

where β is a random number; x_{best} indicates the coordinate of the near best solution found so far throughout all artificial agents; and $x_i^{t_R}$ represents the new coordinates of the artificial agent after the operation of the random walk process.

Step 3. **Evaluation**: the fitness of the artificial agents is calculated by the user defined fitness function and updated to the stored near best solution.

Step 4. **Termination**: the termination conditions are checked in order to decide whether to go back to step 2 or terminate the program and output the near best solution.

The fitness function used in the evaluation process is a set of user defined criteria. In other words, the fitness function is a mathematical representation of the solution space, for which the user wants to solve the problem or to get the optimum solution. Hence, a fitness function is designed in the paper to find the common symmetric positive definite matrix and the control force of the controller.

3. Fuzzy modeling of a TLP system by NN-based representation

The momentum equation obtained from the motion of the floating structure is extensively derived from Newton's second law. Assume that the momentum equation of a TLP system can be characterized by the following differential equation

$$M\ddot{\overline{X}}(t) = -M\overline{r}\phi(t) \tag{29}$$

where $\overline{X}(t) = [\overline{x}_1(t), \overline{x}_2(t) \cdots \overline{x}_n(t)] \in R^n$ is an n-vector; $\ddot{\overline{X}}(t)$, $\dot{\overline{X}}(t)$, $\overline{X}(t)$ are the acceleration, velocity, and displacement vectors, respectively. This is only a static model and M is the mass of the system; $M\overline{r}\phi(t)$ is a wave-induced external force which can be expressed as follows

$$M\overline{r}\phi(t) = F_{wx} - F_{TX} \tag{30}$$

where F_{wx} is the horizontal wave force acting on the both sides of the structure; and F_{Tx} is the horizontal component of the static (or the pre-tensioned) tension applied by the tension legs. The static tension is given by $F_{Tx}=f\xi$.

For controller design (Hammami 2001, Jankovic *et al*. 1996, Seibert and Suarez 1990, Sepulchre 2000, Sepulchre *et al*. 1997, Sontag 1989, Sun and Zang 2003), the standard first-order state equation is obtained from Eq. (31) assuming the equation of motion for a shear-type-building modeled by an n-degrees-of-freedom system controlled by actuators and subjected to an external force $\phi(t)$

$$\dot{X}(t) = AX(t) + E\phi(t) \tag{31}$$

where

$$X(t) = \begin{bmatrix} \overline{x}(t) \\ \dot{\overline{x}}(t) \end{bmatrix}, \quad A = \begin{bmatrix} 0 & I \\ -M^{-1}K & -M^{-1}C \end{bmatrix}, \quad E = \begin{bmatrix} 0 \\ -\overline{r} \end{bmatrix},$$

in which $\overline{X}(t) = [\overline{x}_1(t), \overline{x}_2(t) \cdots \overline{x}_n(t)] \in R^n$ is an n-vector; $\ddot{\overline{X}}(t)$, $\dot{\overline{X}}(t)$, $\overline{X}(t)$ are the acceleration, velocity, and displacement vectors, respectively; matrices M, C, and K are $(n \times n)$

mass, damping, and stiffness matrices, respectively; $\bar{r}$ is an n-vector denoting the influence of the external force; $\phi(t)$ is the excitation with a upper bound $\phi_{up}(t) \geq \|\phi(t)\|$; U(t) corresponds to the actuator forces (generated via active a tendon system or an active mass damper, for example). This is only a static model and $X(t)$ is a $2n$ state vector; A is a $2n \times 2n$ system matrix (Kawamoto *et al*. 1992a, b, Ma and Sun 2001, Takagi and Sugeno 1985).

A neural-network-based model can is described as follows

$$\dot{X}(t) = \Psi^S(W^S \Psi^{S-1}(W^{S-1}\Psi^{S-2}(\cdots\cdots \Psi^2(W^2\Psi^1(W^1\Lambda(t)))\cdots\cdots))) \tag{32}$$

where $\Lambda^T(t)=[X^T(t) \quad U^T(t)]$, with $X^T(t)=[x_1(t) \quad x_2(t) \ldots x_\delta(t)]$. We assume S layers and each layer has R^σ (σ=1,2,...,S) neurons, in which $x_1(t)\sim x_\delta(t)$ and $u_1(t)\sim u_m(t)$ are the input variables. The notation $\boldsymbol{W}^\sigma$ denotes the weight matrix of the σth (σ=1,2,...S) layer. The transfer function vector of the σ^{th} layer is defined as $\Psi^\sigma(v)\equiv[T(v_1) \quad T(v_2) \ldots T(v_{R^\sigma})]^T$.

An LDI system can be described in the state-space representation (Hu 2008; Liu and Li 2010) as follows

$$\dot{Y}(t) = A(a(t))Y(t), \qquad A(a(t)) = \sum_{i=1}^{r} h_i(a(t))\overline{A}_i \tag{33}$$

where r is a positive integer; $a(t)$ is a vector signifying the dependence of $h_i(\cdot)$on its elements, i.e., $h_i(a(t))\equiv h_i(a_1(t), a_2(t)..., a_n(t))$, $a(t)=[a_1(t), a_2(t),..., a_n(t)]^T$ (In general, $a(t)$ coincides with the state vector $X(t)$; $\overline{A}_i$ (i=1,2,...,r) are constant matrices; and $Y(t)=[y_1(t) \quad y_2(t) \ldots y_j(t)]^T$.

According to the interpolation method and Eq. (32), we can obtain

$$\dot{X}(t) = [\sum_{\varsigma^S=1}^{2} h_{\varsigma^S}(t) G_\varsigma^S (W^S[\cdots[\sum_{\varsigma^2=1}^{2} h_{\varsigma^2}(t) G_\varsigma^2 (W^2[\sum_{\varsigma^1=1}^{2} h_{\varsigma^1}(t) G_\varsigma^1 (W^1\Lambda(t))])]\cdots])]$$

$$= \sum_{\varsigma^S=1}^{2}\cdots\sum_{\varsigma^2=1}^{2}\sum_{\varsigma^1=1}^{2} h_{\varsigma^S}(t)\cdots h_{\varsigma^2}(t) h_{\varsigma^1}(t) G_\varsigma^S W^S \cdots G_\varsigma^2 W^2 G_\varsigma^1 W^1 \Lambda(t) = \sum_{\Omega^\sigma} h_{\Omega^\sigma}(t) E_{\Omega^\sigma}\Lambda(t) \tag{34}$$

where

$$\sum_{\varsigma^\sigma} h_{\varsigma^\sigma}(t) \equiv \sum_{q_1^\sigma=1}^{2}\sum_{q_2^\sigma=1}^{2}\cdots\sum_{q_{R^\sigma}^\sigma=1}^{2} h_{q_1^\sigma}(t) h_{q_2^\sigma}(t)\cdots h_{q_{R^\sigma}^\sigma}(t) \text{ for } \sigma = 1, 2, \cdots, S;\ h_{q_\varsigma^\sigma}(t) \in [0\ \ 1],\ \sum_{q_\varsigma^\sigma=1}^{2} h_{q_\varsigma^\sigma}^\sigma(t) = 1$$

for ζ=1,2,...,R^σ, $E_{\Omega^\sigma} \equiv G_\varsigma^S W^S \cdots G_\varsigma^2 W^2 G_\varsigma^1 W^1$, $\sum_{\Omega^\sigma} h_{\Omega^\sigma}(t) \equiv \sum_{\varsigma^S=1}^{2}\cdots\sum_{\varsigma^2=1}^{2}\sum_{\varsigma^1=1}^{2} h_{\varsigma^S}(t)\cdots h_{\varsigma^2}(t) h_{\varsigma^1}(t)$.

Finally, based on Eq. (33), the dynamics of the NN model (29) can be rewritten as the following LDI state-space representation

$$\dot{X}(t) = \sum_{i=1}^{r} h_i(t)\overline{E}_i\Lambda(t) \tag{35}$$

where $h_i(t)\geq 0$; $\sum_{i=1}^{r} h_i(t) = 1$; r is a positive integer; and $\overline{E}_i$ is a constant matrix with an appropriate dimension associated with E_{Ω^σ}. The LDI state-space representation (30) can be further rearranged as follows

$$\dot{X}(t) = \sum_{i=1}^{r} h_i(t)\{A_i X(t)\} \tag{36}$$

where A_i is the partitions of E_i corresponding to the partition $\Lambda(t)$.

Based on the above modeling schemes for the NN-based approach, the nonlinear structural system (31) can be approximated as an LDI representation (36). The LDI representation follows the same rules as the T-S fuzzy model, which combines the flexibility of fuzzy logic theory and the rigorous mathematical analysis tools of a linear system theory into a unified framework. To ensure the stability of the TLP system, the T-S fuzzy model and the stability analysis are recalled. First, the ith rule of the T-S fuzzy model, representing the structural system, can be represented as follows:

$$\begin{aligned} &\text{Rule } i: \text{IF } \ x_1(t) \text{ is } M_{i1} \text{ and} \cdots \text{and } x_p(t) \text{ is } M_{ip} \\ &\text{THEN } \ \dot{X}(t) = A_i X(t) + \overline{A}_i X(t-\tau) + E_i \phi(t) \end{aligned} \tag{37}$$

where i=1,2,...,r and r is the rule number; $X(t)$ is the state vector; M_{ip} (p=1,2,...,g) are the fuzzy sets and $x_1(t)$~$x_p(t)$ are the premise variables. Through using the fuzzy inference method with a singleton fuzzifier, product inference, and center average defuzzifier, the dynamic fuzzy model (36) can be expressed as follows

$$\dot{X}(t) = \frac{\sum_{i=1}^{r} w_i(t)[A_i X(t) + \overline{A}_i X(t-\tau) + E_i \phi(t)]}{\sum_{i=1}^{r} w_i(t)} \tag{38}$$

$$= \sum_{i=1}^{r} h_i(t)(A_i X(t) + \overline{A}_i X(t-\tau) + E_i \phi(t) \tag{39}$$

with

$$w_i(t) = \prod_{p=1}^{g} M_{ip}(x_p(t)) \tag{40}$$

$$h_i(t) = \frac{w_i(t)}{\sum_{i=1}^{r} w_i(t)} \tag{41}$$

where $M_{ip}(x_p(t))$ is the grade of membership of $x_p(t)$ in M_{ip}. It is assumed that

$$w_i(t) \geq 0 \tag{42}$$

$$\sum_{i=1}^{r} w_i(t) > 0 \tag{43}$$

$$\sum_{i=1}^{r} h_i(t) > 0 \tag{44}$$

for all t. Eq. (38) can be easily reformulated as Eq. (39) by defining Eqs. (40)-(41). The delay in the mathematical formula implies the reflection of the wave in the real world.

Definition 2 (Hu 2008): The solutions of a dynamic system are said to be uniformly ultimately bounded (UUB) if there exist positive constants β and κ, and for every $\delta \in (0, \kappa)$ there is a positive constant $T=T(\delta)$, such that

$$\|x(t_0)\| < \delta \Rightarrow \|x(t)\| \le \beta, \forall t \ge t_0 + T . \tag{45}$$

According to the stability concepts above, a stability condition is derived below to guarantee the stability of the system (39).

Before a typical stability condition for fuzzy system (39) is proposed, some useful inequalities are given:

Lemma 1 (Hu 2008): For any A, $B \in \boldsymbol{R}^n$ and for any symmetric positive definite matrix $G \in \boldsymbol{R}^{n\times n}$ or $\boldsymbol{R}$, we have $-2A^TB \le A^TGA + B^TG^{-1}B$.

Theorem 1: The time-delay NN-fuzzy system (39) is stable in the large if there exist common positive definite matrices P_1, P_2,..., P_r and positive constant η such that inequality $\left|\dot{h}_\rho(t)\right| \le \phi_\rho$ is satisfied and

$$\sum_{\rho=1}^{r} \phi_\rho P_\rho \; + A_j P_i + P_i A_j \; + R + P_i \overline{A}_j R^{-1} \overline{A}_j^T P_i + \frac{1}{\eta^2} P_i E_j E_j^T P_i + Q < 0 \tag{46}$$

with $P_i = P_i^T > 0$, for $i, j, l = 1, 2, \cdots, r$.

Proof: Using the fuzzy Lyapunov function candidate for the fuzzy system (39)

$$V(X(t)) = \sum_{i=1}^{r} h_i(t) X^T(t) P_i X(t) + \int_0^\tau X^T(t-\tau) R X(t-\tau) d\tau . \tag{47}$$

The time derivative of V is

$$\begin{aligned}
\dot{V}(X(t)) = & \sum_{\rho=1}^{r} \dot{h}_\rho(t) X^T(t) P_\rho X(t) + \sum_{i=1}^{r} h_i(t) \left\{ \dot{X}^T(t) P_i X(t) + X^T(t) P_i \dot{X}(t) \right\} \\
& + X^T(t) R X(t) - X^T(t-\tau) R X(t-\tau) \\
= & \sum_{\rho=1}^{r} \dot{h}_\rho(t) X^T(t) P_\rho X(t) \\
& + \sum_{i=1}^{r} h_i(t) \left\{ \left[\sum_{j=1}^{r} \sum_{l=1}^{r} h_j(t) h_l(t) \left[A_j X(t) + \overline{A}_j X(t-\tau) \right] + E_j \phi(t) \right]^T P_i X(t) \right.
\end{aligned}$$

$$+ X^T(t)P_i\left[\sum_{j=1}^{r}\sum_{l=1}^{r} h_j(t)h_l(t)[A_jX(t)+\overline{A}_jX(t-\tau)]+E_j\phi(t)\right]\Bigg\}$$

$$+\sum_{i=1}^{r}\sum_{l=1}^{r} h_i(t)h_l(t)\left[X^T(t)RX(t)-X^T(t-\tau)RX(t-\tau)\right]$$

Based on Lemma 1 and the equation listed above, we get

$$\dot{V}(X(t)) \le \sum_{\rho=1}^{r}\dot{h}_\rho(t)X^T(t)P_\rho X(t)+X^T(t)[P_i\overline{A}_j R^{-1}\overline{A}_j^T P_i+\frac{1}{\eta^2}P_iE_jE_j^TP_i]X(t)+\eta^2\left\|\phi_{up}(t)\right\|^2$$

$$+\sum_{i=1}^{r}\sum_{j=1}^{r}\sum_{l=1}^{r} h_i(t)h_j(t)h_l(t)X^T(t)\{A_jP_i+P_iA_j+R\}X(t) \tag{48}$$

$$\le \sum_{i=1}^{r}\sum_{j=1}^{r}\sum_{l=1}^{r} h_i(t)h_j(t)h_l(t)X^T(t)\Bigg\{\sum_{\rho=1}^{r}\phi_\rho P_\rho+A_jP_i+P_iA_j+R$$

$$+P_i\overline{A}_j R^{-1}\overline{A}_j^T P_i+\frac{1}{\eta^2}P_iE_jE_j^TP_i\Bigg\}X(t)+\eta^2\left\|\phi_{up}(t)\right\|^2. \tag{49}$$

Based on Theorem 1, the proof is thereby completed.
The above condition implies that the TLP system is UUB stable under arbitrary excitation.

4. The experiment design and the simulation result

As the same as other nonlinear time-delay systems, a TLP system can be modeled by the NN based fuzzy rules. Moreover, the system parameters including the common positive defined matrix P and the control force matrix K are obtained simultaneously using EBA in the next stage. The obtained system parameters must ensure that the whole system is stable in the large. An inverted pendulum system is taken as an example of the nonlinear system in the simulation. In order to decrease the design complexity, the number of employed rules is minimized. The system is revealed in Fig. 3, where $\Phi(t)$ denotes the rotation angle of the pendulum, and $u(t)$ represents the control force from the controller.

The system is able to be modeled by Eq. (50) from the dynamics

$$\frac{d}{dt}\begin{bmatrix}x_1\\x_2\end{bmatrix}=\begin{bmatrix}0 & 1\\-9 & -6\end{bmatrix}\begin{bmatrix}x_1\\x_2\end{bmatrix}+\begin{bmatrix}0\\9r\end{bmatrix} \tag{50}$$

where x_1 is the radius of the pendulum vertically, x_2 represents the rotation velocity, and r indicates the demand output angle. A set of NN based fuzzy rules is employed to describe the temporary state of the nonlinear system. Similar operations can be found in previous studies (Liu and Lin 2012, Liu and Lin 2013, Liu and Zhang 2003). By combining the whole set of fuzzy rules, the approximation of the nonlinear system is completed. Thus, the fuzzy model approximated inverted pendulum nonlinear system can be described as follows

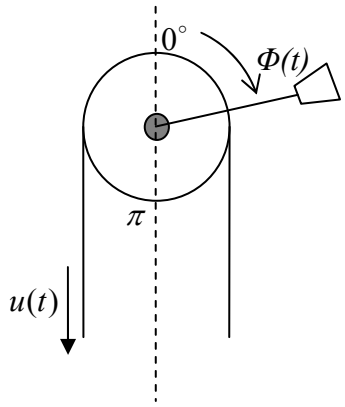

Fig. 3 An inverted pendulum system

$$\textbf{Rule 1:}\ \text{IF}\ \ x_1 \geq \frac{\pi}{3}\ \ \text{(rad), THEN}\ \ \dot{x} = A_1\tilde{x} + B_1 u \tag{51}$$

$$\textbf{Rule 2:}\ \text{IF}\ \ x_1 \approx \frac{\pi}{90}\ \ \text{(rad), THEN}\ \ \dot{x} = A_2\tilde{x} + B_2 u \tag{52}$$

where $A_1 = \begin{bmatrix} 0 & 1 \\ 9.81 & -2 \end{bmatrix}$, $A_2 = \begin{bmatrix} 0 & 1 \\ -5 & -3 \end{bmatrix}$, $B_1 = \begin{bmatrix} 0 \\ -10 \end{bmatrix}$, $B_2 = \begin{bmatrix} 0 \\ -0.081 \end{bmatrix}$, and $\tilde{x} = \begin{bmatrix} \sin x_1 \\ x_2 \end{bmatrix}$.

According to **theorem 1** described in section 3, it provides a useful criterion in Eq. (46) that ensures the system response is stable in the large. Base on **theorem 1**, selecting the proper common positive definite matrix P and the control force K becomes the key problem to be dealt with. In this paper, we use EBA to discover the proper solutions. In this case, the obtained solutions can be classified into two categories: feasible and infeasible. It means that desiging the fitness function in a binary operation form is a simpler way to answer to the need of this application. In this paper, the fitness function is designed based on the stability criterion derived from the LMI conditions via the Lyapunov function approach. The AND logical operation is employed in the fitness function for examining the solutions to produce the binary classification results on the discovered solutions. The fitness function is formulated as follows

$$F = \begin{cases} 1, & \text{if } \Theta < 0 \text{ and } P = P^T > 0. \\ 0, & \text{otherwise.} \end{cases} \tag{53}$$

where F is the fitness value and Θ is given as follows.

$$\Theta = (A_i - B_i K)^T P + P(A_i - B_i K) \tag{54}$$

The matrix P is always constrained to be symmetric when using EBA to adjust the elements

Table 1 Parameters for EBA

Boundary condition for matrix P and K	[−3, 3]
Medium Material	Air
Number of Run	30
Population size	16
Number of Iteration	500

inside it. In addition, a boundary condition is used at the initialization process for both matrices P and K. The matrix P is kept influencing by the same range of boundary conditions for producing feasible solutions in a suitable range. However, the limitation is not applied for the matrix K because the total effect contributed to the whole system by the control force is relatively small. All parameters used in our experiment for EBA are listed in Table 1.

Like other swarm intelligence algorithms and evolutionary methods, EBA requires the recursive operation to find the near best solutions. Thus, the same experiment should be repeated many times to test whether the convergence results are consistent. The number of run listed in Table 1 aims to provide a series of experimental results for examining by statistical methods. In this paper, we choose a fixed iteration number to be the termination criterion. The media material for the transmission of the sound wave is chosen to be air because it fits the natural environment of which the bat lives in. In addition, the population size indicates the number of artificial agents simultaneously exist in the solution space in every iteration. A large population size provides a larger chance for the algorithm to find the near best solutions. However, a larger population size requires more memory resource and computation power. Hence, we set the population size to be 16 in the experiment. The number of feasible solutions obtained by EBA in different runs are shown in Fig. 4.

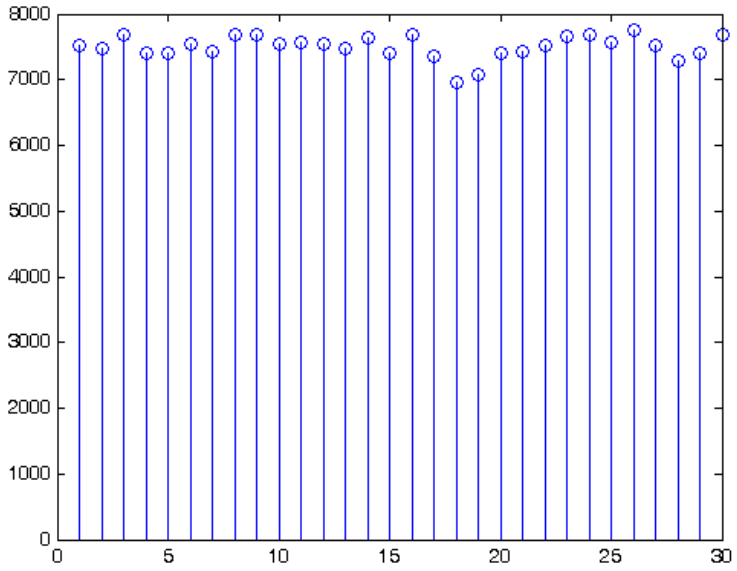

Fig. 4 Number of feasible solutions obtained by EBA in 30 runs

Table 2 Statistical analysis of the obtained feasible solutions

Mean	7502
Minimum	6950
Maximum	7758
Mode	7404
Standard Deviation (STD)	180.7580

Table 3 Samples of the obtained feasible solutions by EBA with system eigen values

	Matrices P and K	Eigen Values	
		with A_1, B_1	with A_2, B_2
Set 1	$P=\begin{bmatrix}3.2641 & 0.6081\\ 0.6081 & 0.9971\end{bmatrix}$, $K^{\mathrm{T}}=\begin{bmatrix}-1.4172\\ -0.1151\end{bmatrix}$	$\begin{bmatrix}-8.1912\\ -2.1826\end{bmatrix}$	$\begin{bmatrix}-9.2384\\ -1.7674\end{bmatrix}$
Set 2	$P=\begin{bmatrix}3.8752 & 0.3773\\ 0.3773 & 1.0645\end{bmatrix}$, $K^{\mathrm{T}}=\begin{bmatrix}-1.6726\\ -0.2747\end{bmatrix}$	$\begin{bmatrix}-12.9525\\ -1.6175\end{bmatrix}$	$\begin{bmatrix}-7.6539\\ -1.9006\end{bmatrix}$
Set 3	$P=\begin{bmatrix}3.9862 & 0.6328\\ 0.6328 & 0.3880\end{bmatrix}$, $K^{\mathrm{T}}=\begin{bmatrix}-1.6705\\ -0.2633\end{bmatrix}$	$\begin{bmatrix}-9.1133\\ -1.9422\end{bmatrix}$	$\begin{bmatrix}-6.5002\\ -1.0776\end{bmatrix}$
Set 4	$P=\begin{bmatrix}3.4095 & 0.3250\\ 0.3250 & 0.5086\end{bmatrix}$, $K^{\mathrm{T}}=\begin{bmatrix}-1.4341\\ -0.0744\end{bmatrix}$	$\begin{bmatrix}-2.9977\\ -2.0886\end{bmatrix}$	$\begin{bmatrix}-3.3554\\ -2.3777\end{bmatrix}$
Set 5	$P=\begin{bmatrix}4.6075 & 0.6311\\ 0.6311 & 0.7700\end{bmatrix}$, $K^{\mathrm{T}}=\begin{bmatrix}-1.4033\\ -0.3754\end{bmatrix}$	$\begin{bmatrix}-9.0082\\ -3.9219\end{bmatrix}$	$\begin{bmatrix}-6.8969\\ -2.9625\end{bmatrix}$
Set 6	$P=\begin{bmatrix}4.4938 & 0.6361\\ 0.6361 & 1.4047\end{bmatrix}$, $K^{\mathrm{T}}=\begin{bmatrix}-1.4631\\ -0.7790\end{bmatrix}$	$\begin{bmatrix}-29.3484\\ -3.0169\end{bmatrix}$	$\begin{bmatrix}-11.5857\\ -2.2598\end{bmatrix}$
Set 7	$P=\begin{bmatrix}3.0719 & 0.0864\\ 0.0864 & 0.9208\end{bmatrix}$, $K^{\mathrm{T}}=\begin{bmatrix}-1.4645\\ -1.9464\end{bmatrix}$	$\begin{bmatrix}-39.6258\\ -0.5657\end{bmatrix}$	$\begin{bmatrix}-6.3168\\ -0.2100\end{bmatrix}$
Set 8	$P=\begin{bmatrix}2.7318 & 0.2748\\ 0.2748 & 0.3832\end{bmatrix}$, $K^{\mathrm{T}}=\begin{bmatrix}-1.3799\\ -1.4559\end{bmatrix}$	$\begin{bmatrix}-13.1626\\ -1.1711\end{bmatrix}$	$\begin{bmatrix}-2.8163\\ -1.8329\end{bmatrix}$
Set 9	$P=\begin{bmatrix}2.1372 & 0.4420\\ 0.4420 & 0.3884\end{bmatrix}$, $K^{\mathrm{T}}=\begin{bmatrix}-1.7609\\ -0.9665\end{bmatrix}$	$\begin{bmatrix}-13.6180\\ -1.4539\end{bmatrix}$	$\begin{bmatrix}-4.9761\\ -1.0774\end{bmatrix}$
Set 10	$P=\begin{bmatrix}1.9452 & 0.1138\\ 0.1138 & 0.4373\end{bmatrix}$, $K^{\mathrm{T}}=\begin{bmatrix}-1.3655\\ 0.0301\end{bmatrix}$	$\begin{bmatrix}-1.2705\\ -0.8623\end{bmatrix}$	$\begin{bmatrix}-2.6596\\ -0.8972\end{bmatrix}$

The statistical analysis of the results obtained by EBA over 30 runs is given in Table 2. Although the STD of the obtained feasible solution in every run is a bit large, the number of found feasible solutions is still much more than enough to decide the system parameters in the application.

According to the experimental results, EBA produces 7,502 feasible solutions in average. Assuming that every artificial agent allocates a feasible solution successfully in all iterations, the maximum number of feasible solutions that can be found in one run is 8,000. This implies that the

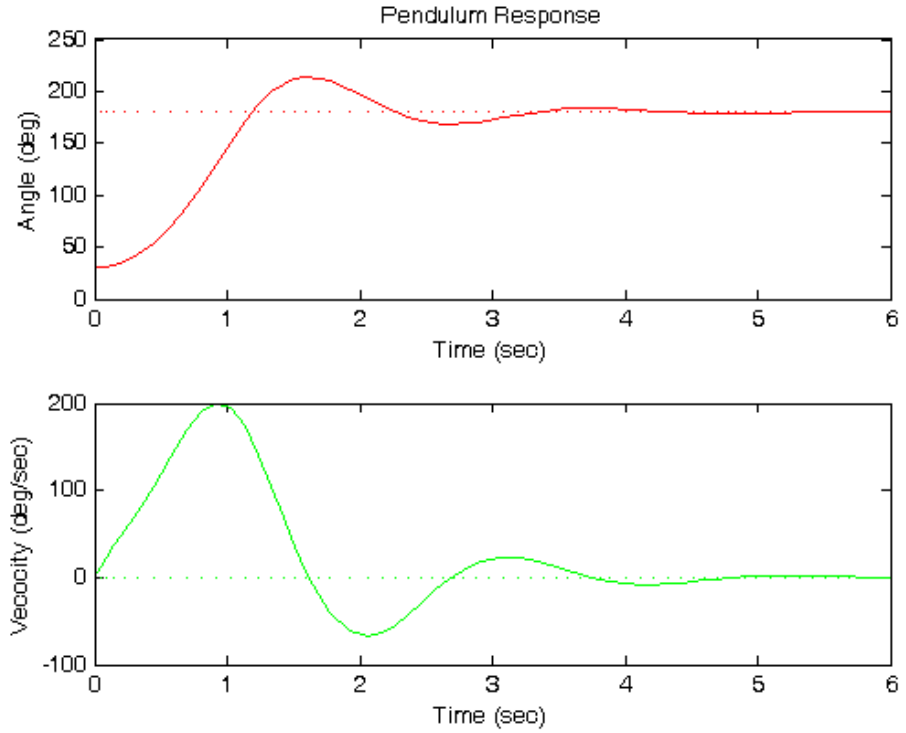

Fig. 5 The angle and the velocity response of the inverted pendulum system without control

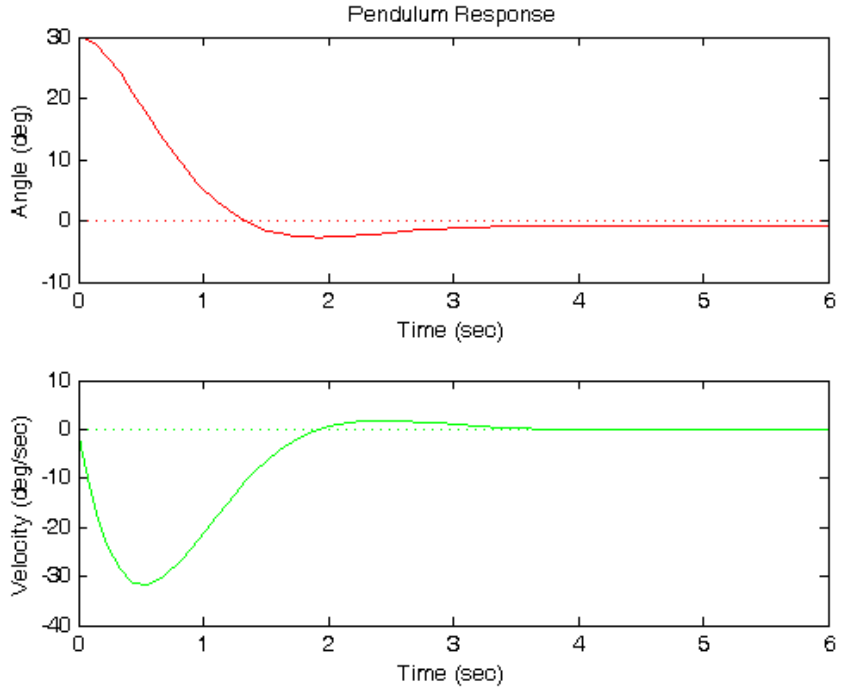

Fig. 6 The controlled inverted pendulum system response by the designed controller

success rate for utilizing the EBA to find feasible solutions is 93.77% in average. The solutions found by the EBA are determined as feasible if the eigen values of Eq. (54) are all negative, because the negative eigen values result in the control system staying stable in the large. Table 3 shows 10 samples from overall feasible solutions found by EBA with the corresponding eigen values.

Fig. 5 shows the changes of the angle and the velocity of the inverted pendulum system without any control force. The initial angle is set to $\pi/6$ (rad) with 0 initial velocity. The simulation time is 6 seconds.

Fig. 6 gives the simulation result controlled by the designed controller. As shown in Fig. 5, without any control, the inverted pendulum would drop to 180° and directly pointing to the ground. On the other hand, the controller maintains the system to be held in the stable state.

5. Conclusions

Currently, fuzzy logic control utilizing artificial intelligent methodology is being actively investigated in for application in the area of robotics. Neural networks (NN) with their powerful learning capability are being sought to create the foundation for many adaptive control systems where on-line adaptation algorithms can be implemented. Fuzzy logic control on the other hand has been proved useful in many rather popular control system applications to provide a rule-based structure. In this article we reviewed the intelligent and robotic algorithm approaches and the proposed a novel neural-network based approach for TLP systems. For the stability analysis, linear matrix inequality (LMI) conditions are derived via fuzzy Lyapunov theory to guarantee the stability and automated design of a TLP system. EBA is utilized to determine the system parameters for the controller. A simulation of the nonlinear inverted pendulum system is given at the last. The experimental result indicates that EBA with our proposed fitness function presents a 93.77 % success rate in average for finding the feasible solutions.

References

Buss, M. and Hashimoto, H. (1996), "Intelligent control for human-machine systems", *IEEE-ASME Tran. Mech*., **1**, 50-55.

Chang, J.F., Yang, T.W. and Tsai, P.W. (2014), "Stock portfolio construction using evolved bat algorithm", *Proceedings of 27th International Conference on Industrial, Engineering & Other Applications of Applied Intelligent Systems*, Kaohsiung, Taiwan, June.

Chang, J.F., Tsai, P.W., Chen, J.F. and Hsiao, C.T. (2014), "The comparison between IABC with EGARCH in foreign exchange rate forecasting", *Proceedings of 1st Euro-China Conference on Intelligent Data Analysis and Applications*, Shenzhen, China, June.

Chu, S.C. and Tsai, P.W. (2007), "Computational intelligence based on behaviors of cats", *Int. J. Innov. Comput. Inform. Control*, **3**(1), 163-173.

Chu, S.C., Tsai, P.W. and Pan, J.S. (2006), "Cat swarm optimization", *Proceedings of Trends in Artificial Intelligence, 9th Pacific Rim International Conference on Artificial Intelligence*, Guilin, China.

Eberhart, R. and Kennedy, J. (1995), "A new optimizer using particle swarm theory", *Proceedings of the 6th International Symposium on Micro Machine and Human Science*, 39-43.

Egresits, C., Monostori, L. and Hornyak, J. (1998), "Multistrategy learning approaches to generate and tune fuzzy control structures and their application in manufacturing", *J. Intel. Manuf*., **9**, 323-329.

Grauel, A., Ludwig, L.A. and Klene, G. (1997), "Comparison of different intelligent methods for process and quality monitoring", *Int. J. Approx. Reason.*, **16**, 89-117.
Hammami, M.A. (2001), "Global convergence of a control system by means of an observer", *J. Optim. Theor. Appl*., **108**, 377-388.
Hu, Q. (2008), "Sliding mode maneuvering control and active vibration damping of three-axis stabilized flexible spacecraft with actuator dynamics", *Nonlin. Dyn*., **52**, 227-248.
Ignaciuk, P. and Bartoszewicz, A. (2010), "Linear-quadratic optimal control strategy for periodic-review inventory systems", *Automatica*, **46**(12), 1982-1993.
Jankovic, M., Sepulchre, R. and Kokotovic, P.V. (1996), "Constructive Lyapunov stabilisation of nonlinear cascade systems", *IEEE Trans. Autom. Control*, **41**, 1723-1735.
Karaboga, D. (2005), "An idea based on honey bee swarm for numerical optimization", Technical Report-TR06, Erciyes University, Engineering Faculty, Computer Engineering Department.
Karaboga, D. and Basturk, B. (2008), "On the performance of artificial bee colony (ABC) algorithm", *Appl. Soft Comput*., **8**(1), 687-697.
Kawamoto, S., Tada, K., Onoe, N., Ishigame, A. and Taniguchi, T. (1992), "Construction of exact fuzzy system for nonlinear system and its stability analysis", *Proceedings of 8th Fuzzy System Symposium*, Hiroshima, Japan.
Kawamoto, S., Tada, K., Ishigame, A. and Taniguchi, T. (1992), "An approach to stability analysis of second order fuzzy systems", *Proceedings of IEEE International Conference on Fuzzy Systems*, San Diego, CA, 1427-1434.
Korkmaz, S. (2011), "A review of active structural control: challenges for engineering informatics", *Comput. Struct.*, **89**(23), 2113-2132.
Kuo, R.J. and Xue, K.C. (1998), "An intelligent sales forecasting system through integration of artificial neural network and fuzzy neural network", *Comput. Indus.*, **37**, 1-15.
Kuok, S.C. and Yuen, K.V. (2012), "Structural health monitoring of Canton tower using Bayesian framework", *Smart Struct. Syst.*, **10**(4-5), 375-391.
Lam, H.K. (2009), "Stability analysis of T-S fuzzy control systems using parameter-dependent Lyapunov function", *IET Control Theor. Appl*., **3**, 750-762.
Lee, H.H. and Juang, H.H. (2012), "Experimental study on the vibration mitigation of offshore tension leg platform system with UWTLCD", *Smart Struct. Syst.*, **9**(1), 71-104.
Lee, H.J., Park, J.B. and Chen, G. (2001), "Robust fuzzy control of nonlinear systems with parameter uncertainties", *IEEE Trans. Fuzzy Syst*., **9**, 369-379.
Lewandowski, R., Bartkowiak, A. and Maciejewski, H. (2012), "Dynamic analysis of frames with viscoelastic dampers: a comparison of damper models", *Struct. Eng. Mech.*, **41**(1), 113-137.
Lian, S.T., Marzuki, K. and Rubiyah, Y. (1998), "Tuning of a neuro-fuzzy controller by genetic algorithms with an application to a coupled-tank liquid-level control system", *Eng. Appl. Artif. Intel.*, **11**, 517-529.
Liu, S.C. and Lin, S.F. (2012), "LMI-based robust sliding control for mismatched uncertain nonlinear systems using fuzzy models", *Int. J. Rob. Nonlin. Control*, **22**(16), 1827-1836.
Liu, S.C. and Lin, S.F. (2012), "LMI-based robust adaptive control for mismatched uncertain nonlinear time-delay systems using fuzzy models", *Proceedings of 2012 International symposium on Computer, Consumer and Control*, Taichung, Taiwan, 552-555.
Liu, S.C. and Lin, S.F. (2013), "Robust sliding control for mismatched uncertain fuzzy time-delay systems using linear matrix inequality approach", *J. Chin. Inst. Eng.*, **36**(5), 589-597.
Liu, X. and Zhang, Q. (2003), "New approach to H1 controller designs based on fuzzy observers for T-S fuzzy systems via LMI", *Automatica*, **39**, 1571-1582.
Liu, Y.J. and Li, Y.X. (2010), "Adaptive fuzzy output-feedback control of uncertain SISO nonlinear systems", *Nonlin. Dyn*., **61**, 749-761.
Loria, A. and Nesic, D. (2003), "On uniform boundedness of parametrized discrete-time systems with decaying inputs: applications to cascades", *Syst. Control Lett*., **94**, 163-174.
Ma, X.J. and Sun, Z.Q. (2001), "Analysis and design of fuzzy reduceddimensional observer and fuzzy functional observer", *Fuzz. Set. Syst*., **120**, 35-63.

Mazenc, F., Sepulchre, R. and Jankovic, M. (1999), "Lyapunov functions for stable cascades and applications to stabilisation", *IEEE Trans. Automat. Contr*., **44**, 1795-1800.
Narendra, K.G., Khorasani, K. and Sood, V.K. *et al*. (1998), "Intelligent current controller for an HVDC transmission link", *IEEE Tran. Power Syst.*, **13**, 1076-1083.
Panda, G., Pardhan, P.M. and Majhi, B. (2011), "IIR system identification using cat swarm optimization", *Exp. Syst. Appl.*, **38**, 12671-12683.
Panteley, E. and Loria, A. (1998), "On global uniform asymptotic stability of nonlinear time-varying non autonomous systems in cascade", *Syst. Control Lett*., **33**, 131-138.
Pardhan, P.M. and Panda, G. (2012), "Solving multiobjective problems using cat swarm optimization", *Exp. Syst. Appl.*, **39**, 2956-2964.
Park, J., Kim, J. and Park, D. (2003), "LMI-based design of stabilizing fuzzy controllers for nonlinear systems described by Takagi-Sugeno fuzzy model", *Fuzz. Set. Syst*., **122**, 73-82.
Sciortino, J.C. (1997), "Autonomous ESM systems", *Nav. Eng. J.*, **109**, 73-84.
Shi, Y. and Fang H. (2010), "Kalman filter-based identification for systems with randomly missing measurements in a network environment", *Int. J. Control*, **83**(3), 538-551.
Seibert, P. and Suarez, R. (1990), "Global stabilisation of nonlinear cascade systems", *Syst. Control Lett*., **14**, 347-352.
Sepulchre, R. (2000), "Slow peaking and low-gain designs for global stabilisation on nonlinear systems", *IEEE Tran. Autom. Control*, **45**, 453-461.
Sepulchre, R., Jankovic, M. and Kokotovic, P.V. (1997), *Constructive Nonlinear Control, Series in Communications and Control Engineering*, Springer, Berlin.
Simoes, M.G., Bose, B.K. and Spiegel, R.J. (1997), "Design and performance evaluation of a fuzzy-logic-based variable-speed wind generation system", *IEEE Tran. Indus. Appl.*, **33**, 956-965.
Sontag, E.D. (1989), "Remarks on stabilisation and input-to-state stability", *Proceedings of the 28th IEEE Conference on Decision Control*, Tampa, FL, 1376-1378.
Sontag, E.D. (1988), "Smooth stabilization implies coprime factorization", *IEEE Tran. Automat. Contr*., **34**, 435-443.
Sontag, E.D. and Wang, Y. (1995), "On characterizations of the inputto-state stability property", *Syst. Control Lett*., **24**, 351-359.
Sun, Q., Li, R. and Zhang, P. (2003), "Stable and optimal adaptive fuzzy control of complex systems using fuzzy dynamic model", *Fuzzy Sets Syst*., **133**, 1-17.
Takagi, T. and Sugeno, M. (1985), "Fuzzy identification of systems and its applications to modeling and control", *IEEE Tran. Syst. Man Cybern*., **15**, 116-132.
Tanaka, K., Ikeda, T. and Wang, H.O. (1996), "Robust stabilization of a class of uncertain nonlinear systems via fuzzy control: quadratic stability, H∞ control theory, and linear matrix inequalities", *IEEE Tran. Fuzz. Syst*., **4**, 1-13.
Tanaka, K. and Sano, M. (1994), "On the concepts of regulator and observer of fuzzy control systems", *Third IEEE international Conference on Fuzzy Systems*, Orlando, FL, 767-772.
Tsai, P.W., Kham, M.K., Pan, J.S. and Liao, B.Y. (2012), "Interactive artificial bee colony supported passive continuous authentication system", *IEEE Syst. J.*, **8**(2), 395-405..
Tsai, P.W., Pan, J.S., Liao, B.Y., Tsai, M.J. and Vaci, I. (2012), "Bat algorithm inspired algorithm for solving numerical optimization problems", *Appl. Mech. Mater.*, **148-149**, 134-137.
Tyan, C.Y., Wang, P.P. and Bahler, D.R. (1996), "An application on intelligent control using neural network and fuzzy logic", *Neurocomput*., **12**, 345-363.
Wang, H.O., Tanaka, K. and Griffin, M. (1996), "An approach to fuzzy control of nonlinear systems: stability and design issues", *IEEE Tran. Fuzz. Syst*., **4**, 14-23.
Wang, Z.H., Chang, C.C., and Li, M.C. (2012), "Optimizing least-significant-bit substitution using cat swarm optimization strategy", *Inform. Sci.*, **192**, 98-108.
Yen, G.G. (1996), "Health monitoring of vibration signatures in rotorcraft wings", *Neur. Proc. Lett.*, **4**, 127-137.
Yu, L. and Giurgiutiu, V. (2005), "Advanced signal processing for enhanced damage detection with

piezoelectric wafer active sensors", *Smart Struct. Syst.*, **1**(2), 185-215.
Zhu, Y., Zhang, Q., Wei, Z. and Zhang, L. (2013), "Robust stability analysis of Markov jump standard genetic regulatory networks with mixed time delays and uncertainties", *Neurocomput.*, **110**(13), 44-50.

CC